NRC Research Press

ARTICLE

# Theoretical study of phenol and hydroxyl radical reaction mechanism in aqueous medium by the DFT/B3LYP/6-31+G(d,p)/CPCM model

Pavithra Bhakthi Jayathilaka, Gayani Chathurika Pathiraja, Athula Bandara, Nalaka Deepal Subasinghe, and Nadeeshani Nanayakkara

**Abstract:** Four different possible reaction pathways of phenol and hydroxyl radical reaction were investigated theoretically by density functional theory (DFT) B3LYP with the 6-31+G(d,p) calculations under the conductor-like polarized continuum model (CPCM). According to frontier molecule orbital theory, both the highest occupied orbital and lowest occupied orbital of phenol (25th orbital) showed −602.79 and −43.53 kJ mol$^{-1}$ molecular orbital energies, respectively. This resulted in a 559.27 kJ mol$^{-1}$ relative energy gap. Relative energies of the ortho product radical (o-PR) (i.e., −54.08 kJ mol$^{-1}$) was lower than those of both the para product radical (p-PR) (−50.03 kJ mol$^{-1}$) and the meta product radical (m-PR) (−47.10 kJ mol$^{-1}$). Then, o-PR was found to be the energetically most stable product radical. The ortho addition reaction path was confirmed as the most possible reaction path and its major intermediate was found as catechol with 99.09% product distribution. Percentages of hydroquinone, resorcinol, and phynoxyl radicals in the system were found as 0.053%, 0.029%, and 0.009%, respectively.

*Key words:* phenol, hydroxyl radicals, density functional theory (DFT), polarized continuum model.

**Résumé :** Quatre différentes voies réactionnelles de la réaction des radicaux phénol et hydroxyle ont été étudiées de manière théorique à l'aide de calculs effectués au niveau B3LYP/6-31+G(d,p) de la théorie de la fonctionnelle de la densité (TFD) sous le modèle du continuum polarisable apparenté à un conducteur (« conductor like polarized continuum model » ou CPCM). Selon la théorie de l'orbitale moléculaire frontière, les orbitales haute occupée et basse vacante du phénol (25$^{e}$ orbitale) ont respectivement des énergies d'orbitale moléculaire égales à −602,79 et −43,53 kJ mol$^{-1}$. Il en a résulté une bande d'énergie relative de 559,27 kJ mol$^{-1}$. L'énergie relative du produit radicalaire ortho (o-PR) (égale à −54,08 kJ mol$^{-1}$) était plus basse que celles des produits radicalaires para (p-PR) (−50,03 kJ mol$^{-1}$) et méta (m-PR) (−47,10 kJ mol$^{-1}$). Par la suite, il a mis en évidence qu'o-PR était le produit radicalaire énergétiquement le plus stable. L'addition en ortho a été confirmée comme étant la voie réactionnelle la plus probable, son intermédiaire réactionnel majoritaire étant le catéchol dont le pourcentage était de 99,09 %. Les pourcentages d'hydroquinone, de résorcinol et de radicaux phénoxyles dans le système réactionnel étaient respectivement de 0,053 %, 0,029 % et 0,009 %. [Traduit par la Rédaction]

*Mots-clés :* phénol, radicaux hydroxyles, théorie de la fonctionnelle de la densité (TFD), modèle du continuum polarisable.

## Introduction

Phenol ($C_6H_5OH$) is one of the major organic water pollutants. Sixteen million tons of phenol is produced per year by various industrial applications, such as refineries, coking operations, coal processing, and manufacturing of petrochemicals.[1–5] Since it causes significant health effects on humans (i.e., the ingestion of 1 g of phenol can kill a person) and its aqueous form is more toxic, destruction of phenol through a water treatment technique is important.[1,5,6–8] But the mechanisms associated with hydroxyl radicals of phenol in water medium are complex. Moreover, its intermediates can be more harmful than the parent compound. Therefore, the understanding of the intermediate products and possible reaction pathways is necessary prior to implementation of any water treatment technique. Although phenol has been extensively studied as a model compound, these studies are mainly focused on reactions in air medium. A detailed theoretical study on the phenol degradation mechanism in water medium under the conductor-like polarized continuum model (CPCM) is still needed.[9,10]

The purpose of this paper is to fill this gap by modelling the phenol and hydroxyl radical reaction mechanism in water medium under the CPCM. The mechanism study focused on the characterization of reaction properties by the frontier molecule orbital theory. Then, the stability of transition states and reaction complexes was calculated by relative molecular energies in aqueous medium. Finally, the primary intermediates with their product distributions were predicted. To do that, four different possible reaction pathways were investigated theoretically by density functional theory (DFT). The Becke-style 3-parameter Lee–Yang–Parr correlation hybrid function (B3LYP) with the 6-31+G (d,p) basis set was involved in the calculations.[11–13] The conductor-like screening model, a type of polarized continuum model,[14,15] was utilised to study the aqueous medium effect on the molecules as the solvation method.[14,16]

## Computational methods

The reaction between phenol and $\dot{O}H$ radicals was modelled using Gaussian 03 software.[17] As the methodology, the DFT and

Received 22 April 2014. Accepted 9 June 2014.

**P.B. Jayathilaka, G.C. Pathiraja, and N.D. Subasinghe.** Institute of Fundamental Studies, Kandy, Sri Lanka.
**A. Bandara.** Department of Chemistry, University of Peradeniya, Sri Lanka; Postgraduate Institute of Science, University of Peradeniya, Sri Lanka.
**N. Nanayakkara.** Institute of Fundamental Studies, Kandy, Sri Lanka; Department of Civil Engineering, Faculty of Engineering, University of Peradeniya, Sri Lanka; Postgraduate Institute of Science, University of Peradeniya, Sri Lanka.
**Corresponding author:** Nadeeshani Nanayakkara (e-mail: kgnn@pdn.ac.lk).

Can. J. Chem. **92**: 809–813 (2014) dx.doi.org/10.1139/cjc-2014-0191

CPCM[14,15] were used with B3LYP[11,12] and 6-31+G(d,p) basis set[13] on each of four possible channels (Fig. 1). B3LYP/6-31+G (d,p) was reliable on optimization and frequency calculations and the relatively large basis set, 6-31+G(d,p), reduced the basis set truncation and basis set superposition errors. Geometry optimization calculations were performed on the reactants, product radicals, and prereactive and transition states. Frontier molecule orbital theory was used to study the reaction properties of reactants and optimized structures of phenol and hydroxyl radical. Harmonic frequency calculations were performed on DFT/B3LYP/6-31+G(d,p) to confirm whether the optimized geometries are in local minima or transition states on the potential energy surface. Transition state optimization was done using the Berny optimization method.[18] The solvation model, CPCM, was used on all calculations including reactants, transition states, and product radicals.[14–16,19] The relative energy and rate constant calculations were made at a temperature of 298.15 K and the water medium, with a dielectric constant $\varepsilon = 878.39$.[11]

## Results and discussion

### Characterization of phenol and hydroxyl radical reaction properties

To study the reaction properties of reactants, optimized structures of phenol and hydroxyl radical were considered (i.e.,Fig. 2) with the frontier molecule orbital theory. The highest occupied molecular orbital (HOMO) and the lowest unoccupied molecular orbital (LUMO) of the reactants were computed at the DFT/CPCM/B3LYP/6-31+G(d,p) level as given in Fig. 3. According to the calculation, the hydroxyl radical has an oxygen atom with a lone pair of electrons at the p orbital. Similarly, molecular orbitals of phenol were described by 163 molecular coefficients. Its 25th orbital is the HOMO. As mentioned in the frontier molecule orbital theory, the greatest electron density is occupied at the HOMO orbital and electrophilic reactions may take place by attacking at this position. Its 26th virtual orbital is the LUMO. The HOMO and LUMO orbitals of phenol have −602.79 and −43.53 kJ mol$^{-1}$ molecular energy, respectively. The energy gap between them is 559.27 kJ mol$^{-1}$. These energies reflect the chemical activity of phenol. While LUMO represents the role of electron acceptor, HOMO represents the electron donor. There, the HOMO, HOMO-1, and HOMO-2 are mainly focused on the p orbitals of the phenol ring (Fig. 3).

### Calculations in the aqueous phase

For the confirmation of the transition structures, vibration frequency data are needed. Frequency calculations (i.e., DFT/B3LYP/6-31+G(d,p)) were performed on optimized geometries of transition states and reactant complexes. Moreover, thermodynamic data[20] of each species were obtained from frequency calculations.

#### *Transition state and reactant complexes*

A transition state was identified by having one imaginary frequency, while the reactant and reactant complexes do not have imaginary frequencies. There are four possible product radicals depending on the predicted reaction channels such as the ortho addition product radical (o-PR), para addition product radical (p-PR), meta addition product radical (m-PR), and hydrogen abstraction product radical. For example, the optimized geometries of possible product radicals are shown in Fig. 4. According to the obtained results, for o-PR, its C–C bond length of the ortho addition site was increased after adding hydroxyl radical to the phenol ring. It was increased by 1.499 and 1.506 Å for C4–C5 and C3–C4, respectively. This was due to partial transfer of the electron density of the aromatic ring to the newly formed C–O bond. Therefore, there is enhancement of the σ character. Thus, the values of bond lengths corresponding to C5–C6 and C2–C3 bonds lie between the values of σ and π bond lengths. It shortened the C5–C6 and C2–C3 bonds by 0.03 and 0.02 Å, respectively. The same pattern was shown by both p-PR and m-PR product radicals. For p-PR, the C1–C2 and C6–C1 bond lengths were 1.502 and 1.502 Å, respectively. Its C2–C3 and C5–C6 bonds were shortened after formation of the new C–O bond. The C1–C2 and C2–C3 bond lengths of m-PR were observed as 1.502 and 1.502 Å, respectively. Its C6–C1 and C3–C4 shortened bond lengths were 1.372 and 1.368 Å, respectively.

**Fig. 1.** Four possible reaction paths of the phenol and hydroxyl radical reaction.

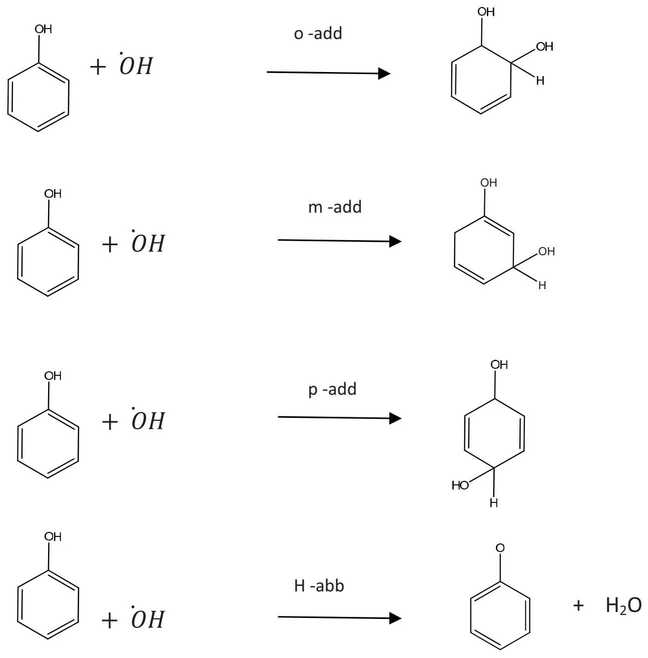

Optimized structures of transition states and reactant complexes were identified. Their relative free energies were computed relative to the energy of reactants as follows:

$$(1) \qquad E_{\text{relative}} = E(\text{X}) - E(\text{reactants})$$

where $E(\text{X})$ is the energy of reactants, the energy of a transition state, or the energy of a product radical.

Ortho addition transition states had the lowest relative energy and hydrogen abstraction transition states had the highest energy (Table 1). Since the product radicals of addition reactions can form hydrogen bonds in aqueous medium, they are more stable than the hydrogen abstraction reaction product radical. h-PR showed comparatively high energy and it was less stable than the addition-type product radicals. The result showed that tk;1the energy of o-PR is lower than that of both p-PR and m-PR. It was −50.03 kJ mol$^{-1}$ for p-PR and −47.10 kJ mol$^{-1}$ for m-PR. This was 4 and 6.98 kJ mol$^{-1}$ higher, respectively, than the o-PR value of −54.08 kJ mol$^{-1}$. Therefore, o-PR was the most stable product radical among them.

According to relative free energy calculations (i.e., Fig. 5), the hydrogen abstraction reaction path is the least possibe in aqueous medium (i.e., relative energy of $\approx 2 \times 10^5$ kJ mol$^{-1}$). But, addition reaction paths had some possibility of occurring compared with the abstraction reaction. However, final results showed that the ortho addition path was the most possible reaction path among the addition reaction paths.

In addition, based on these frequency analyses, activationtk;1 energy and rate constant calculations were performed. These calculations were used to predict the primary intermediates and product distribution. To calculate relative activation energies ($E_a$), the energy difference between the transition state (TS) and the reactant was considered:

**Fig. 2.** Optimized geometries of reactants, prereactant complexes from calculations, along with selected bond distances (Å) and bond angles (°). Some experimental values are given in parentheses.

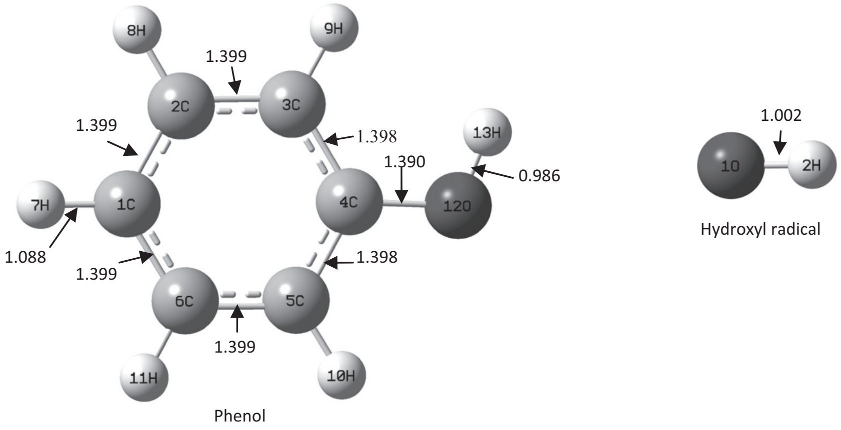

**Fig. 3.** Optimized geometries of reactant HOMO and LUMO analysis: (*a*) LUMO diagram of phenol, (*b*) HOMO diagram of phenol, (*c*) HOMO-1 diagram of phenol, (*d*) HOMO-2 diagram of phenol, (*e*) LUMO diagram of the hydroxyl radical, and (*f*) HOMO diagram of the hydroxyl radical.

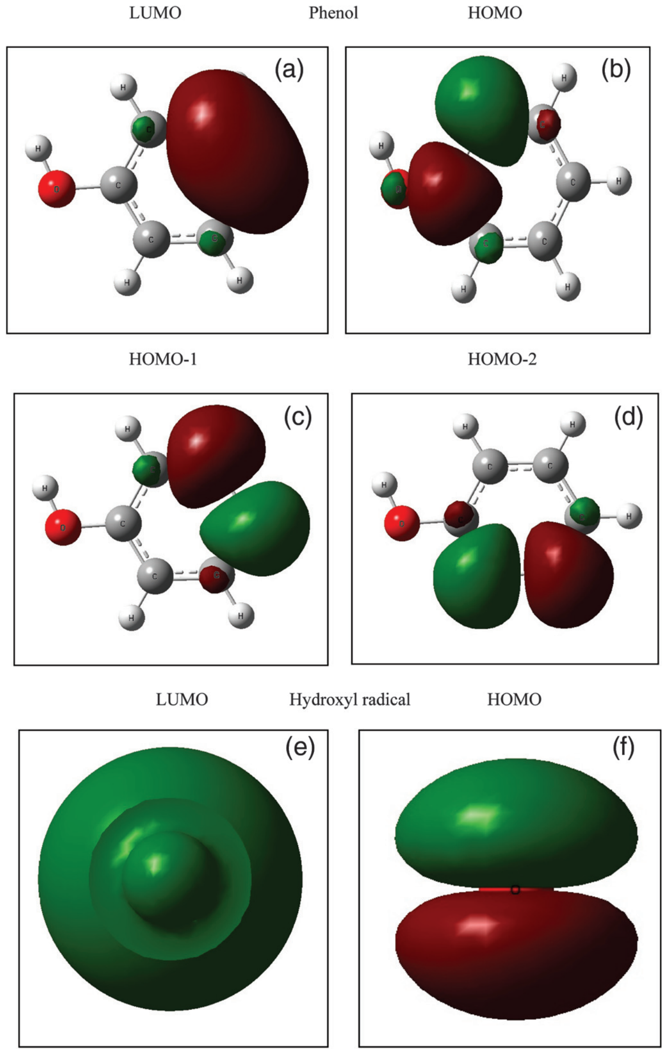

$$E_a = E(\text{TS}) - E(\text{reactants}) \tag{2}$$

In the case of difficulties in confirming the transition state, bond dissociation energy was used to estimate the activation energy as follows:[21]

$$E_{\text{bond dissociation}} = E(C_6H_5\dot{O}) + E(\dot{O}H) - E(\text{product}) = E_a \tag{3}$$

where $E_a$ is the activation energy and $E$ is the zero-point energy corrected energy of reactants and product radicals.

According to these calculations (eq. 2), the ortho and para reaction paths showed negative activation energy, –20.83 and –0.26 kJ mol$^{-1}$, respectively. This implies that both reactions are barrierless and their rates of reaction have been decreased. Since the reactants already have sufficient energy to initiate the reaction, they occur spontaneously. Between ortho and para reactions, the ortho reaction has a greater possibility of occurring due to its higher negative activation energy (Table 2).

### *Theoretical prediction of primary intermediates and product distribution*

Theoretically possible four reaction paths also end up with primary intermediate products. Ortho addition ends up with catechol, para addition with hydroquinone, and meta addition with resorcinol.

The presence of those intermediates in the system was predicted through rate constants and product distribution calculations. Transition state theory was used to obtain the absolute rate constants at 298.15 K temperature as follows:[22,23]

$$k(298, H) = \frac{k_b T}{h} e^{-\left(\frac{\Delta G^{\#}}{RT}\right)} \tag{4}$$

where $k_b$ is Boltzmann's constant, $h$ is Planck's constant, $\Delta G^{\#}$ is the activation free energy at 298 K and the standard state of 1 mg dm$^{-3}$, $R$ is the gas constant, and $T$ is absolute temperature.[23] Based on the above transition state theory equation (eq. 4), thermodynamic data of transition states and reactants were used for rate constant calculations. Activation free energies (reaction energy barriers) (i.e., using the DFT/B3LYP/6-31+G(d,p) method) were estimated using relative energies of reactant and transition states while including zero-point energy correction.[12] In addition, the tunnelling corrections to the reaction paths with the negative activation energies were not applied while calculating their rate

**Fig. 4.** Optimized geometries of product radicals from calculations, along with selected bond distances (Å): (*a*) o-PR, (*b*) m-PR, (*c*) p-PR, and (*d*) h-PR.

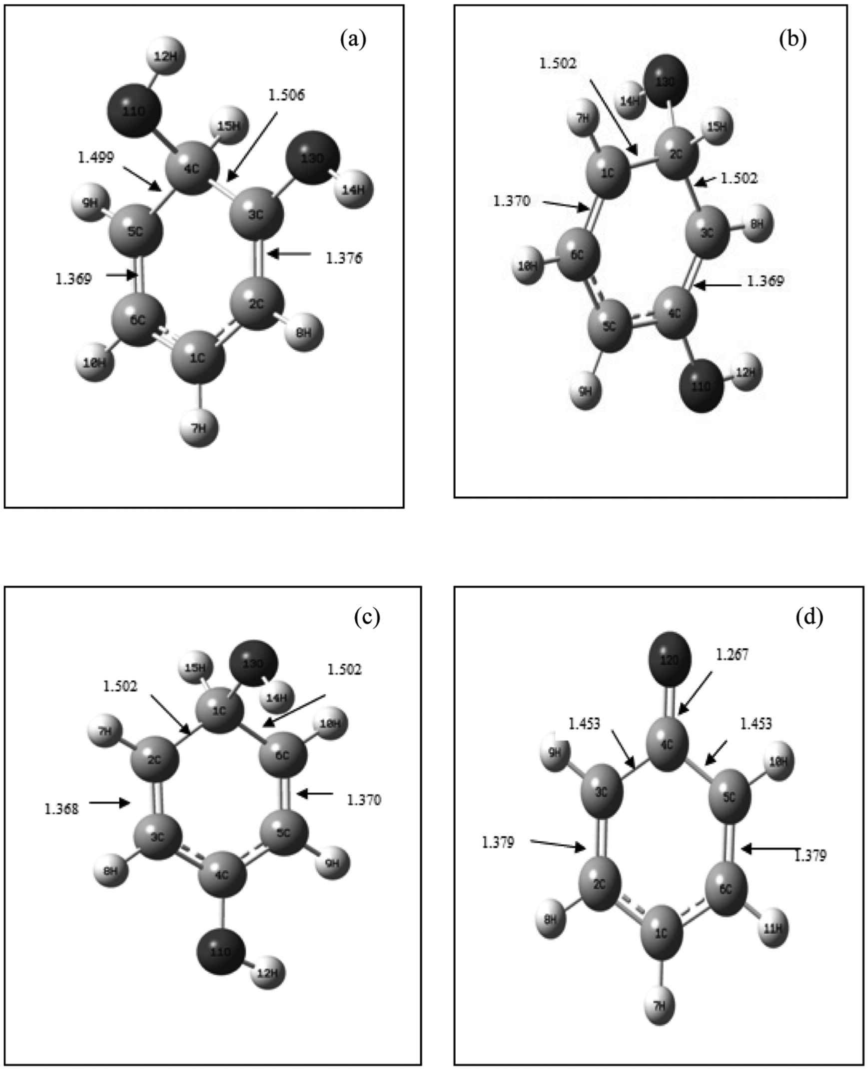

**Table 1.** Calculated relative energies (kJ mol$^{-1}$) of the phenol and hydroxyl radical reaction (computed at zero collision energy).

| Reaction path | Reactants | Transition state | Product radical |
|---|---|---|---|
| Ortho addition | 0.00 | −20.83 | −54.08 |
| Para addition | 0.00 | −0.26 | −50.08 |
| Meta addition | 0.00 | 1.31 | −47.10 |
| H abstraction | 0.00 | 1.58 | 200532.45 |

constants. Relative rate constants were predicted through the Arrhenius equation[22] as follows:

$$k = Ae^{\left(-\frac{E_a}{RT}\right)} \tag{5}$$

where $k$ is the rate constant, $A$ is a pre-exponential factor, $E_a$ is the activation energy, $R$ is the gas constant, and $T$ is absolute temperature (i.e., 298.15 K for this system). Since all of these reaction paths are similar, a preexponential factor was assumed to be the same for all reactions. Then, relative energies were predicted through Arrhenius equation ratios while using relative activation energy values.

**Fig. 5.** Relative free energy diagram of four possible reaction paths.

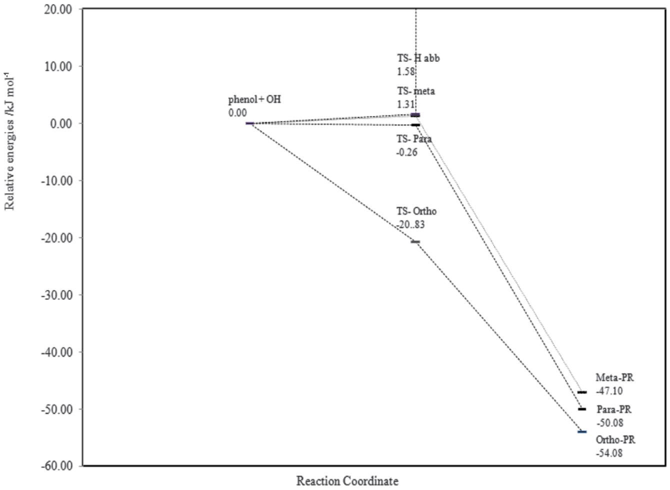

**Table 2.** Calculated rate constants and product branching ratios (%) in the phenol and hydroxyl radical reaction (computed at zero collision energy).

| Reaction path | Product | Rate constant | Branching ratio |
|---|---|---|---|
| Ortho addition | Catechol | $8.57\times10^{-13}$ | 99.908 |
| Para addition | Hydroquinone | $9.13\times10^{-14}$ | 0.053 |
| Meta addition | Resorcinol | $2.52\times10^{-14}$ | 0.029 |
| Hydrogen abstraction | Phenoxyl radical | $1.60\times10^{-16}$ | 0.009 |

The resulting rate constant values are given in Table 2. The results of those two calculations suggested that the ortho addition path and hydrogen abstraction path have the highest rate and the lowest rate, respectively. The relative rate constant calculation results showed that there was a geater possibility of forming ortho products (i.e., catechol) than hydrogen abstraction path products in water medium. When considering only the above possible four reaction paths, the presence of catechol in this medium was 90 times higher than the para products (hydroquinone). Meta products (resorcinol) were 87 times less than ortho products. Similarly, product branching ratios were calculated based on transition state theory rate constant values and are shown in Table 2.

Product branching ratios were calculated by dividing each species' corresponding rate constant by the overall rate constant while considering the total number of similar addition sites.[24] Based on product branching ratio calculations, catechol showed 99.908% availability. Therefore, catechol is the main intermediate product available in the system. The percentages of hydroquinone, resorcinol, and phynoxyl radicals in the system are 0.053%, 0.029%, and 0.009%, respectively.

## Conclusion

This theoretical work has helped us to understand the intermediate products and possible reaction pathways of the phenol with hydroxyl radical reaction.

According to the frontier molecular orbital theory, the aromatic ring of phenol has a higher possibility of reaction due to its high electron density. As a result, the highly electrophilic hydroxyl radical can attack the aromatic ring easily. Therefore, from the nature of the HOMO and LUMO of the reactants, it was concluded that the addition reaction was the most favourable reaction in the given conditions. Further, relative energy calculations confirmed that the ortho position of the ring was more active towards hydroxyl radicals.

Secondly, relative rate constant calculation results showed that the ortho product (i.e., catechol) has a greater possibility of forming in water medium than the other three products. Therefore, it was concluded that the amount of catechol in the system was 90 times as much as the para product hydroquinone. At the same time, it was shown that meta products resorcinol were 87 times less than ortho products. Subsequently, branching ratio calculations confirmed the above findings with available percentage values: 99.908% catechol, 0.053% hydroquinone, 0.029% resorcinol, and 0.009% phynoxyl radicals.

Finally, this study concluded that the main mechanism of phenol and hydroxyl radical reaction in water medium is more favourable in the ortho addition reaction path (i.e., made catechol as primary intermediate). The meta addition path is the least favourable among them. The findings of this study can be used as a guide prior to implementation of any water treatment technique.

## Acknowledgement

The authors acknowledge the Institute of Fundamental Studies, Sri Lanka, the University of Peradeniya,Sri Lanka, and and International Foundation for Science, Sweden (grant No. W 5336/1).

## References

(1) Busca, G.; Berardinelli, S.; Resini, C.; Arrighi, L. *J. Hazard. Mater.* **2008**, *160* (2–3), 265. doi:10.1016/j.jhazmat.2008.03.045.
(2) Song, S.; Zhan, L.; He, Z.; Lin, L.; Tu, J.; Zhang, Z. *J. Hazard. Mater.* **2010**, *175*, 614. doi:10.1016/j.jhazmat.2009.10.051.
(3) Comninellis, C.; Pulgarin, C. *J. Appl. Electrochem.* **1991**, *21*, 703. doi:10.1007/BF01034049.
(4) San, N.; Hatipoglu, A.; Kocturk, G.; Cinar, Z; *J. Photochem. Photobiol. A* **2002**, *146*, 189. doi:10.1016/S1010-6030(01)00620-7.
(5) Li, M.; Feng, C.; Hu, W.; Zhang, Z.; Sugiura, N. *J. Hazard. Mater.* **2009**, *162*, 455. doi:10.1016/j.jhazmat.2008.05.063.
(6) Kingsland, S.; Kjellstrom, T.; Lodh, M.; McMichael, T.; Ranmuthugala, G.; Shrestha, R. *Disease Control Priorities in Developing Countries*; World Bank: Oxford University Press, UK. 2006.
(7) Ma, H.; Zhang, X.; Ma, Q.; Wang, B. *J. Hazard. Mater.* **2009**, *165* (1–3), 475. doi:10.1016/j.jhazmat.2008.10.012.
(8) Kanu, I.; Achi, O. K. *J. Appl. Sci. Tech. Environ. Sanit.* **2011**, *1*, 75.
(9) Cartaxo, M. A.; Ablad, K.; Douch, J.; Berghoute, Y.; Hamdani, M.; Mendonca, M. H.; Nogueira, J. M. F.; Pereira, M. I. S. *Chemosphere* **2012**, *86* (4): 341. doi:10.1016/j.chemosphere.2011.09.040.
(10) Martínez-Huitle, C. A.; Andrade, L. S. *Quim. Nova* **2011**, *34*, 850. doi:10.1590/S0100-40422011000500021.
(11) McFerrin, C. A.; Hall, R. W.; Dellinger, B. *J. Mol. Struct. THEOCHEM* **2008**, *848*, 16. doi:10.1016/j.theochem.2007.09.005.
(12) Huang, X.; Liu, C.; Huang, J.; Li, H. *Comp. Theor. Chem.* **2011**, *976* (2011), 51. doi:10.1016/j.comptc.2011.08.001.
(13) Song, L.; Yu, F.; Wu, L.-X.; Zhou, X.-G.; Liu, S.-L. *Acta Phys. Chim. Sin.* **2011**, *27*, 801. doi:10.3866/PKU.WHXB20110409.
(14) Pfaendtner, J.; Broadbelt, L. J. *Chem. Eng. Sci.* **2007**, *62*, 5232. doi:10.1016/j.ces.2006.12.080.
(15) Tomasi, J.; Bonaccorsi, R.; Cammi, R.; Valle, F. J. O. *J. Mol. Struct. THEOCHEM* **1991**, *234*, 401. doi:10.1016/0166-1280(91)89026-W.
(16) Fortunelli, A.; Tomasi, J. ; *Chem. Phys. Lett.* **1994**, *231*, 34. doi:10.1016/0009-2614(94)01253-9.
(17) Frisch, M. J.; Trucks, G. W.; Schlegel, H. B.; Scuseria, G. E.; Robb, M. A.; Cheeseman, J. R.; Montgomery, J. A.; Vreven, T.; Kudin, K. N.; Burant, J. C.; Millam, J. M.; Iyengar, S. S.; Tomasi, J.; Barone, V.; Mennucci, B.; Cossi, M.; Scalmani. G.; Rega, N.; Petersson, G. A.; Nakatsuji, H.; Hada, M.; Ehara, M.; Toyota, K.; Fukuda, R.; Hasegawa, J.; Ishida, M.; Nakajima, T.; Honda, Y.; Kitao, O.; Nakai, H.; Klene, M.; Li, X.; Knox, J. E.; Hratchian, H. P.; Cross, J. B.; Adamo, C.; Jaramillo, J.; Gomperts, R.; Stratmann, R. E.; Yazyev, O.; Austin, A. J.; Cammi, R.; Pomelli, C.; Ochterski, J. W.; Ayala, P. Y.; Morokuma, K.; Voth, G. A.; Salvador, P.; Dannenberg, J. J.; Zakrzewski, V. G.; Dapprich, S.; Daniels, A. D.; Strain, M. C.; Farkas, O; Malick, D. K.; Rabuck, A. D.; Ragha-vachari, K.; Foresman, J. B.; Ortiz, J. V.; Cui, Q.; Baboul, A. G.; Clifford, S.; Cioslowski, J.; Stefanov, B. B.; Liu, G.; Liashenko, A.; Piskorz, P.; Komaromi, I.; Martin, R. L.; Fox, D. J.; Keith, T.; Al-Laham, M. A.; Peng, C. Y.; Nanayakkara, A.; Challacombe, M.; Gill, P. M. W.; Johnson, B.; Chen, W.; Wong, M. W.; Gon-zalez, C; Pople, J. A. *Gaussian 03, Rev. A.1*; Gaussian, Inc.: Pittsburgh, PA, 2003.
(18) Farkas, O.; Schlegel, H. B. *J. Mol. Struct. THEOCHEM* 2003, *666–667*, 31. doi:10.1016/j.theochem.2003.08.010.
(19) Stevic, M. C.; Ignjatovic, L. M.; Ciric-Marjanovic, G.; Marjanovic, J. B.; Zima, J. *J. Electroanal. Chem.* 2012, *677–680*, 69. doi:10.1016/j.jelechem.2012.04.030.
(20) Jalbout, A. F.; Nazari, F.; Turker, L. ; *J. Mol. Struct. THEOCHEM* **2004**, *671*, 1. doi:10.1016/S0166-1280(03)00347-6.
(21) Jarvis, M. W.; Daily, J. W.; Carstensen, H. H.; Dean, A. M.; Sharma, S.; Dayton, D. C.; Robichaud, D. J.; Nimlos, M. R. *J. Phys. Chem. A* **2011**, *115*, 428. doi:10.1021/jp1076356.
(22) Young, D. C. *Computational Chemistry: A Practical Guide for Applying Techniques to Real World Problems*, 1st ed.; John Wiley & Sons, Inc.: Hoboken, NJ, 2001.
(23) Baptista, L.; Silva, E. C.; Arbilla, G. ; *J. Mol. Struct. THEOCHEM* **2008**, *851*, 1. doi:10.1016/j.theochem.2007.09.027.
(24) Hatipoglu, A.; Vione, D.; Yaclcin, Y.; Minero, C.; Cinar, Z. *J. Photochem. Photobiol. A* **2010**, *215*, 59. doi:10.1016/j.jphotochem.2010.07.021.